



저작자표시-비영리-변경금지 2.0 대한민국

이용자는 아래의 조건을 따르는 경우에 한하여 자유롭게

- 이 저작물을 복제, 배포, 전송, 전시, 공연 및 방송할 수 있습니다.

다음과 같은 조건을 따라야 합니다:



저작자표시. 귀하는 원저작자를 표시하여야 합니다.



비영리. 귀하는 이 저작물을 영리 목적으로 이용할 수 없습니다.



변경금지. 귀하는 이 저작물을 개작, 변형 또는 가공할 수 없습니다.

- 귀하는, 이 저작물의 재이용이나 배포의 경우, 이 저작물에 적용된 이용허락조건을 명확하게 나타내어야 합니다.
- 저작권자로부터 별도의 허가를 받으면 이러한 조건들은 적용되지 않습니다.

저작권법에 따른 이용자의 권리는 위의 내용에 의하여 영향을 받지 않습니다.

이것은 [이용허락규약\(Legal Code\)](#)을 이해하기 쉽게 요약한 것입니다.

[Disclaimer](#)

**The role of sirtuin 2 (SIRT2)  
in hyperoxic acute lung injury**

**Yu Jin Lee**

**The Graduate School  
Yonsei University  
Department of Medical Science**

**The role of sirtuin 2 (SIRT2)  
in hyperoxic acute lung injury**

**A Master's Thesis Submitted  
to the Department of Medical Science  
and the Graduate School of Yonsei University  
in partial fulfillment of the  
requirements for the degree of  
Master's of Medical Science**

**Yu Jin Lee**

**June 2024**

**This certifies that the Master's Thesis  
of Yu Jin Lee is approved.**

---

Thesis Supervisor    Myung Hyun Sohn

---

Thesis Committee Member    Kyung Won Kim

---

Thesis Committee Member    Ho-Geun Yoon

**The Graduate School  
Yonsei University  
June 2024**

## ACKNOWLEDGEMENTS

대학원을 처음 입학했던 순간이 엇그제 같은데, 어느덧 시간이 흘러 졸업을 앞두고 되었습니다. 석사 과정 동안 정말 많은 것들을 배우고 성장해 나갈 수 있었던 것 같습니다. 한 권의 논문이 나올 수 있도록 저에게 많은 영향을 주고 도움을 주셨던 분들에게 감사함을 표하고자 합니다.

먼저, 다양한 실험들을 진행할 수 있게 기회를 주시고 지원해주신 손명현 지도 교수님께 깊은 감사의 말씀을 드립니다. 매주 조언과 격려와 함께 저의 결과를 기다려 주시고, 전문적으로 지도해주신 덕분에 학문적으로 한 걸음 더 성장할 수 있었습니다. 또한, 제 논문을 꼼꼼하고 면밀하게 확인해주시고, 미흡한 부분을 보완할 수 있도록 많은 조언을 주신 김경원 교수님과 윤호근 교수님께도 감사 인사를 드립니다.

다음으로 학위 과정 동안 가장 많은 시간을 함께 보내며 제 연구에 누구보다 신경 써 주시고, 많은 도움을 주신 소아과 연구실 선생님들께 감사 인사를 드립니다. 먼저 실험실 전체를 이끌어주신 김미나 선생님, 많은 실험들을 가르쳐주시고 연구의 방향을 잡는 데 있어 끊임없는 조언과 격려를 해주셔서 감사드립니다. 그리고 고민이 있을 때마다 항상 성심성의껏 들어주시고 아낌없는 조언을 해 주신 은결 선생님께도 감사드립니다. 또, 실험을 하는 데 있어서 가장 중요한 마우스 모델링을 가르쳐 주신 혜린 선생님께도 감사드립니다. 그리고 옆자리에서 궁금한 것이 있을 때마다 흔쾌히 알려주시고 도움을 주신 지수 선생님께도 감사드리며, 항상 실험하면서 어려움이 있을 때마다 같이 고민해주고 도움을 주신 승민 선생님께도 감사드립니다. 마지막으로, 묵묵히 옆에서 실험을 도와준 창현오빠, 실험실을 활기차게 만들어준 주연이와 병찬이 모두 도와줘서 고맙다는 말을 전하며, 남은 학위 과정도 무사히 마치기를 응원하겠습니다. 이처럼 실험실 모든 분들의 도움이 있었기에 제가 논문을 완성할 수 있었고, 석사 과정 동안 정말 많은 것들을 배울 수 있었습니다. 이 지면을 빌려 정말 감사한 마음을 전해보고 싶습니다. 감사합니다.

그리고 학위 과정 동안 정말 많은 힘이 되어준 친구들에게도 고마운 마음을 전하고 싶습니다. 항상 제 곁에서 응원해주고, 힘든 일은 잠시 잊고 마음이 편하도록 의지할

수 있는 곳이 되어주어 고맙습니다. 그리고 항상 약속 일정을 저에게 맞춰 배려해주고, 웃고 떠들며 소중한 시간들을 함께 보내면서 좋은 에너지를 받아 가게끔 해주어 진심으로 고맙습니다.

마지막으로 항상 저의 성장과 학업에 있어서 아낌없이 지원해주신 어머니께 진심으로 감사드립니다. 언제나 옆에서 따뜻한 말과 응원을 해주시고, 무한한 사랑을 주신 덕분에 학위 과정을 잘 마무리할 수 있었습니다. 그리고 항상 힘내라고 맛있는 음식을 보내주시는 외할머니와 대학원 생활을 응원하고 격려해주신 저의 친인척분들께 정말 감사의 말씀을 드립니다.

저의 대학원 생활을 옆에서 지켜봐 주시고 도와주신 모든 분들께 다시 한번 감사드리며, 이 감사한 마음을 잊지 않고 저도 제 곁에 있는 소중한 분들께 힘이 되는 사람이 될 수 있도록 하겠습니다. 진심으로 감사드립니다.

2024년 6월

이유진

## TABLE OF CONTENTS

LIST OF FIGURES	iii
ABSTRACT	iv
1. INTRODUCTION	1
2. MATERIALS AND METHODS	3
2.1. Mice	3
2.2. Hyperoxic exposure	3
2.3. Quantitative real-time polymerase chain reaction (PCR)	3
2.4. Western blot	4
2.5. Histology and immunohistochemistry staining	4
2.6. Bronchoalveolar lavage fluid (BALF) collection and cell count	5
2.7. Bicinchoninic acid (BCA) assay	5
2.8. Enzyme-linked immunosorbent assay (ELISA)	5
2.9. Terminal deoxynucleotidyl transferase dUTP nick end labeling (TUNEL) assay	5
2.10. Lactate dehydrogenase (LDH) assay	6
2.11. Caspase activity	6
2.12. Immunofluorescence staining	6
2.13. Proximity ligation assay (PLA)	7
2.14. AGK2 treatment	7
2.15. Statistical analysis	7
3. RESULTS	9
3.1. SIRT2 expression levels are increased by hyperoxia	9
3.2. The absence of SIRT2 mitigates inflammation in hyperoxic acute lung injury	13
3.3. Deletion of SIRT2 leads to diminished apoptosis	18

3.4. SIRT2 regulates apoptosis by deacetylates FOXO3 in hyperoxic acute lung injury .....	23
3.5. Inhibition of SIRT2 ameliorates hyperoxic acute lung injury .....	28
4. DISCUSSION .....	32
5. CONCLUSION .....	35
REFERENCES .....	36
ABSTRACT IN KOREAN .....	40

## LIST OF FIGURES

<Fig. 1> SIRT2 expression is elevated by hyperoxia .....	10
<Fig. 2> SIRT2 deficiency attenuates inflammation in hyperoxic acute lung injury .....	14
<Fig. 3> The absence of SIRT2 ameliorates apoptosis in hyperoxic acute lung injury .....	19
<Fig. 4> SIRT2 promotes apoptosis through deacetylating FOXO3 .....	24
<Fig. 5> AGK2 improves hyperoxic acute lung injury .....	29
<Fig. 6> SIRT2 mediates FOXO3 deacetylation to promote transcriptional activation of FOXO3 target genes related to apoptosis in hyperoxic acute lung injury .....	31

## ABSTRACT

### The role of sirtuin 2 (SIRT2) in hyperoxic acute lung injury

**Background :** Oxygen therapy is helpful for patients with breathing difficulties, but sustained supplementation of high-concentration oxygen can cause hyperoxic acute lung injury. Sirtuin 2 (SIRT2), a nicotinamide adenine dinucleotide (NAD<sup>+</sup>)-dependent deacetylase, has been shown to be involved in pulmonary fibrosis, apoptosis, and inflammation. However, the contribution of SIRT2 in pathogenesis of hyperoxia-induced acute lung injury is unknown. Therefore, the purpose of this study was to elucidate the role of SIRT2 in hyperoxic acute lung injury.

**Methods :** Wild-type (WT) mice and SIRT2 deficient (SIRT2<sup>-/-</sup>) mice were exposed to room air or hyperoxia for 72 hours. After hyperoxic exposure, changes in hyperoxia-induced inflammation and apoptosis were evaluated in WT and SIRT2<sup>-/-</sup> mice. Then, the involvement of forkhead box O3 (FOXO3) was investigated in altered hyperoxia-induced lung injury in SIRT2<sup>-/-</sup> mice. For the SIRT2 inhibitor study, hyperoxia-induced inflammation and apoptosis was assessed after AGK2 treatment.

**Results :** SIRT2 expression levels were elevated in WT mice after hyperoxic exposure. Total cell counts in bronchoalveolar lavage fluid (BALF), pro-inflammatory cytokine levels, and histological lung injury were significantly attenuated in SIRT2<sup>-/-</sup> mice compared with WT mice following hyperoxic exposure. Under prolonged hyperoxic conditions, survival rates were higher in the absence of SIRT2. Moreover, SIRT2 deficiency led to decreased apoptotic cells, cell cytotoxicity, caspase activities, and expression of pro-apoptotic molecules when exposed to hyperoxia. Furthermore, FOXO3 acetylation was augmented in the absence of SIRT2 after hyperoxic exposure. SIRT2 was also involved in the transcription of apoptosis-related FOXO3 target genes BIM, PUMA, PERP, and AATF. Finally, hyperoxia-induced inflammation and apoptosis was attenuated when administered with AGK2.

**Conclusion :** Taken together, SIRT2 plays a critical role in the pathogenesis of hyperoxic acute lung injury by regulating apoptotic signaling through FOXO3 deacetylation. These findings indicate that SIRT2 can provide a new therapeutic strategy for hyperoxic acute lung injury.

---

Key words : acute lung injury, apoptosis, deacetylation, FOXO3, hyperoxia, SIRT2

## 1. Introduction

Oxygen administration can be used for therapeutic purposes in patients with respiratory failure, such as pneumonia, and chronic obstructive pulmonary disease (COPD). However, prolonged exposure to high concentrations of oxygen can occasionally cause hyperoxic acute lung injury, potentially leading to death in severe cases.<sup>1,2</sup> More than 200,000 cases of acute lung injury occur annually in the United States, with mortality rates reaching 40–50%.<sup>3</sup> In premature infants, they are at risk of hyperoxia-induced lung injury due to long-term use of oxygen, which is one of the most important contributing factors in the development of bronchopulmonary dysplasia (BPD).<sup>4,5</sup> Thus, a better understanding of the underlying mechanisms of hyperoxic acute lung injury is needed to improve the care of patients requiring supplemental oxygen.<sup>4</sup> Hyperoxia triggers the activation of the pro-inflammatory responses, leading to alveolar edema caused by the destruction of capillary endothelium, and alveolar epithelial cell damage and death.<sup>6</sup> Furthermore, excessive oxygen increases reactive oxygen species (ROS), which induces oxidative stress and has direct cytotoxicity.<sup>7</sup> It leads to the disruption of the homeostasis of cellular processes, cause damage to cells and tissues, and induce apoptosis.<sup>7-9</sup> Within the characteristics of hyperoxia, pulmonary cell death through apoptosis is regarded as a crucial element in the pathological aspects of hyperoxia.<sup>5,10-12</sup>

Recent studies indicate that epigenetic modification contributes to hyperoxia.<sup>13-16</sup> Post-translational modifications (PTMs) such as acetylation, methylation, phosphorylation, and ubiquitination are included in epigenetic modifications.<sup>17</sup> Sirtuin 2 (SIRT2), a member of the sirtuin family, is a nicotinamide adenine dinucleotide (NAD<sup>+</sup>)-dependent class III protein deacetylase.<sup>18,19</sup> SIRT2 is the sole sirtuin protein predominantly located in the cytoplasm, but capable of shuttling between the cytosol and the nucleus.<sup>20</sup> Many studies have shown that SIRT2 plays various roles in oxidative stress, inflammation, apoptosis, autophagy, and metabolism.<sup>19,21-23</sup> SIRT2 exhibits robust deacetylase activity among the sirtuins, and is capable of deacetylating both histone and non-histone proteins.<sup>18,24</sup> One of the major targets of SIRT2 is forkhead box O3 (FOXO3), also known as FOXO3a, a transcription factor characterized by a conserved fork head DNA-binding domain.<sup>25</sup> FOXO3 mediates various cellular processes by inducing the transcription of target genes associated with apoptosis, proliferation, DNA damage,

survival, and cell cycle progression.<sup>26</sup> Numerous studies have shown that various PTMs alter the transcriptional activity of FOXO3, and affect changes in the expression of target genes, DNA binding, and subcellular localization.<sup>26-29</sup>

This study hypothesized that SIRT2 can exert an influence on hyperoxic acute lung injury through its deacetylase properties. To achieve it, this research established hyperoxia-induced acute lung injury model by exposure to >95% oxygen for 72 hours, and compared hyperoxia-induced responses in wild-type (WT) and SIRT2 deficient (SIRT2<sup>-/-</sup>) mice to evaluate the impact of SIRT2 on hyperoxia. Using an inhibitor of SIRT2, the impact on SIRT2 in hyperoxic acute lung injury was further confirmed.

## 2. Materials and methods

### 2.1. Mice

All experiments utilized male mice aged 6–8 weeks. WT C57BL/6 mice were purchased from Orient Bio Inc. (Seongnam, Korea). SIRT2<sup>-/-</sup> C57BL/6 mice were kindly provided by Dr. Hyun-Seok Kim (Ewha Womans University, Seoul, Korea). The animals used in the experiment were housed under specific pathogen-free conditions, and maintained on a 12-hour light-dark cycle. Studies were approved by the Institutional Animal Care and Use Committee (IACUC) at Yonsei University (protocol no. 2020-0296; Seoul, Korea).

### 2.2. Hyperoxic exposure

WT and SIRT2<sup>-/-</sup> mice were placed in an acrylic chamber (57×42×37 cm<sup>3</sup>; JEUNGDO Bio & Plant Co., Ltd., Seoul, Korea) and supplied with >95% oxygen at 5 L/minutes for 72 hours. To maintain hyperoxic conditions (>95% O<sub>2</sub>), the oxygen level was continuously monitored using an oxygen analyzer (MaxO2<sup>+</sup> A; MAXTEC, Salt, Lake City, UT, USA). Control mice were kept in room air under identical conditions for 72 hours. All mice had *ad libitum* access to food and water during the experiment. After 72 hours, the mice were sacrificed for analysis.

### 2.3. Quantitative real-time polymerase chain reaction (PCR)

To isolate total mRNA, lung tissues were homogenized using a T10 Basic Ultra-Turrax<sup>®</sup> Homogenizer (IKA Labortechnik, Staufen, Germany) with TRIzol reagent. Concentration of mRNA was quantified using a Nanodrop 2000 spectrophotometer (Thermo Fisher Scientific, Waltham, MA, USA) and synthesized cDNA using ReverTra Ace<sup>™</sup> qPCR RT Master Mix (Toyobo Co., Ltd., Osaka, Japan) according to manufacturer's instructions. Quantitative real-time PCR was performed with StepOnePlus<sup>™</sup> Real-Time PCR System (Applied Biosystems, Waltham, MA, USA) using Power SYBR<sup>™</sup> Green PCR Master Mix (Applied Biosystems). The results were analyzed using  $2^{-\Delta\Delta CT}$  method normalized to importin 8 (IPO8) as the housekeeping gene.

## 2.4. Western blot

Protein was extracted from the lung tissues using a homogenizer with Pierce™ RIPA buffer and Halt™ Protease Inhibitor Cocktail at a ratio of 100:1 (both from Thermo Fisher Scientific). Protein concentration was quantified using Bradford protein assay with Bio-Rad Protein Assay Dye Reagent Concentrate (Bio-Rad Laboratories, Hercules, CA, USA). Protein samples were prepared to contain quantified protein using 4X Laemmli Sample Buffer (Bio-Rad Laboratories) and  $\beta$ -mercaptoethanol. Samples were separated by electrophoresis on 10–13.5% SDS polyacrylamide gels and transferred to hydrophobic polyvinylidene fluoride (PVDF) membranes (Millipore, Burlington, MA, USA). After blocking with 5% skim milk, membranes were incubated overnight at 4 °C with primary antibodies against SIRT2 (Proteintech, Rosemont, IL, USA), BAX, cytochrome C, and  $\beta$ -actin (all from Cell Signaling Technology, Beverly, MA, USA). The next day, the membranes were incubated with anti-rabbit secondary antibody conjugated to horseradish peroxidase (Santa Cruz Biotechnology, Dallas, TX, USA). The protein bands were visualized using a chemiluminescent detection reagent and the Amersham™ ImageQuant™ 800 western blot imager (both from Cytiva, Marlborough, MA, USA). The images were analyzed using the Image J software 1.8.0 (National Institutes of Health, Bethesda, MD, USA) and normalized to  $\beta$ -actin.

## 2.5. Histology and immunohistochemistry staining

Lung tissues were fixed in 4% formaldehyde and embedded in paraffin. The paraffin blocks were cut into 5  $\mu$ m sizes and subjected to hematoxylin and eosin staining. For immunohistochemistry staining, paraffin-embedded lung tissue slides were deparaffinized through xylene and then sequentially rehydrated in 100%, 95%, and 70% ethanol. Heat-induced epitope retrieval was performed using a Target Retrieval Solution (Dako, Glostrup, Denmark) through a steamer for 25 minutes followed by cooling down at room temperature for 30 minutes. After washing, the protein blocking process was performed using the Peroxidase Block Solution and the Protein Block Serum-Free Solution (both from Dako). The slides were incubated overnight at 4 °C with the following primary antibodies: SIRT2 (1:200; Proteintech) and anti-rabbit IgG (1:200; Santa Cruz Biotechnology). The next day, the slides were incubated with horseradish peroxidase-labeled polymer anti-rabbit, followed by staining using the Liquid DAB+ Substrate Chromogen System (both from Dako). Finally, lung tissue specimens were

mounted using a Faramount Mounting Medium (Dako), and observed through a BX43 Upright Microscope (Olympus, Tokyo, Japan).

## **2.6. Bronchoalveolar lavage fluid (BALF) collection and cell count**

The trachea of mice was cannulated and the lungs were lavaged twice with 0.9 mL phosphate-buffered saline (PBS). The BALF was centrifuged at 3,000 rpm for 5 minutes at 4 °C to isolate BAL cells and supernatants. Total cell count in BAL cells was measured using Trypan Blue solution. BAL cells were attached to the slides through cytospin centrifuge, and differential cell count was performed using Diff-Quick staining (PanReac AppliChem, Darmstadt, Germany).

## **2.7. Bicinchoninic acid (BCA) assay**

Total protein in BALF was measured using Pierce™ BCA Protein Assay Kits (Thermo Fisher Scientific). BALF supernatants and bovine serum albumin (BSA) protein standards were dispensed into a 96-well plate, followed by the addition of the BCA working reagent. After reacting in an incubator at 37 °C for 30 minutes, the protein concentration was measured using a microplate reader (Molecular Devices, CA, USA) at 562 nm.

## **2.8. Enzyme-linked immunosorbent assay (ELISA)**

The levels of pro-inflammatory cytokines in the BALF of mice were assessed using mouse interleukin (IL)-6, and IL-1 $\beta$  DuoSet ELISA and mouse tumor necrosis factor (TNF)- $\alpha$  Quantikine ELISA kits (all from R&D Systems, Minneapolis, MN, USA) according to the manufacturer's instructions. The concentration was obtained by subtracting 570 nm from 450 nm using a microplate reader (Molecular Devices).

## **2.9. Terminal deoxynucleotidyl transferase dUTP nick end labeling (TUNEL) assay**

TUNEL assay was conducted using the In Situ Cell Death Detection Kit, AP (Roche, Basel, Switzerland). The lung section slides that underwent epitope retrieval were prepared as described above. Protein blocking was performed using the Protein Block Serum-Free Solution

(Dako). TUNEL reaction mixture was added to the lung tissue sections and incubated for 1 hour at 37 °C in a humidified atmosphere. The slides were incubated with a converter-AP reagent for 30 minutes as above, and subsequently stained with the substrate solution. Finally, the sections were mounted using the Faramount Mounting Medium (Dako), and observed through a BX43 Upright Microscope (Olympus).

## **2.10. Lactate dehydrogenase (LDH) assay**

LDH assay was executed using Cytotoxicity Detection Kit<sup>PLUS</sup> (Roche). BALF supernatants and LDH standards were dispensed into a 96-well plate. The catalyst and the dye solution were mixed to prepare the reaction mixture and then added to the plate. After incubation at room temperature for 30 minutes, the reaction was stopped with the stop solution. LDH activity was measured at 492 nm in a microplate reader (Molecular Devices), and additionally measured at 692 nm to subtract the reference wavelength. The percent of cytotoxicity was calculated according to the manufacturer's instructions.

## **2.11. Caspase activity**

Proteins were extracted from the lungs as previously described. The Caspase-Glo<sup>®</sup> assay kit (Promega, Madison, WI, USA) was employed to measure Caspase-3/7, -8, and -9 activities. Protein samples at a concentration of 1 mg/mL were added to a white-walled 96-well plate, then the equal volume of Caspase-Glo<sup>®</sup> Reagents was added and mixed. While incubating at room temperature, the luminescence of each sample was measured using a luminometer at 30-minute intervals from 30 minutes to 3 hours.

## **2.12. Immunofluorescence staining**

The slides containing paraffin-embedded lung tissue were deparaffinized and rehydrated. Epitope retrieval and protein blocking processes were performed as described above. The slides were then incubated with FOXO3 (1:100; Proteintech) and acetyl-FOXO3 (Lys271) (1:200; Affinity Biosciences, Cincinnati, OH, USA) overnight at 4 °C. The next day, sections were incubated at 4 °C for 30 minutes and then at room temperature for 30 minutes with the following secondary antibodies: Alexa Fluor 555-conjugated goat anti-mouse IgG and Alexa Fluor 647-

conjugated donkey anti-rabbit IgG (1:500; both from Abcam, Cambridge, UK). Cell nuclei were stained with 4', 6-diamidino-2-phenylindole (DAPI; Thermo Fisher Scientific) for 2 minutes, followed by mounting the slides using the Faramount Mounting Medium (Dako). Images were captured using a confocal microscope (LSM 780; Zeiss, Oberkochen, Germany) and analyzed using Image J software 1.8.0 (National Institutes of Health).

### **2.13. Proximity ligation assay (PLA)**

In situ PLA analysis (Sigma-Aldrich, St. Louis, MO, USA) was carried out according to the manufacturer's instructions. As previously described, the slides underwent deparaffinization, rehydration and heat-induced epitope retrieval. For protein blocking, the slides were incubated in a heated humidity chamber at 37 °C for 1 hour with Duolink<sup>®</sup> Blocking Solution. SIRT2, FOXO3 (1:100; Both from Proteintech), and p300 (1:100; Abcam) diluted in Duolink<sup>®</sup> Antibody Diluent were added to the slides and incubated overnight at 4 °C. The next day, the slides were incubated in a heated humidity chamber for 1 hour at 37 °C with PLUS and MINUS secondary PLA probes specific to the primary antibody species. Following the application of PLA probes, the probes attached to tissue slides were subjected to ligation and amplification using the supplied reagents. The samples were then mounted using a Duolink<sup>®</sup> In Situ Mounting Media with DAPI and captured using a confocal microscope (LSM 780; Zeiss).

### **2.14. AGK2 treatment**

For the SIRT2 inhibition study, AGK2 (an inhibitor of SIRT2; MedChem Express, Monmouth Junction, NJ, USA) was administered to WT mice via intraperitoneal injection before exposure to hyperoxia. AGK2 (80mg/kg) was sequentially dissolved in 10% dimethyl sulfoxide (DMSO), 40% PEG300, 5% Tween-80 and 45% saline. Control mice were treated identically with DMSO dissolved in PEG300, Tween-80, and saline. Mice were sacrificed after hyperoxic exposure for 72 hours.

### **2.15. Statistical analysis**

All of the statistical analyses were performed with GraphPad Prism 5 software version 5.01 (GraphPad, San Diego, CA, USA). The results represent the mean  $\pm$  standard error of the mean

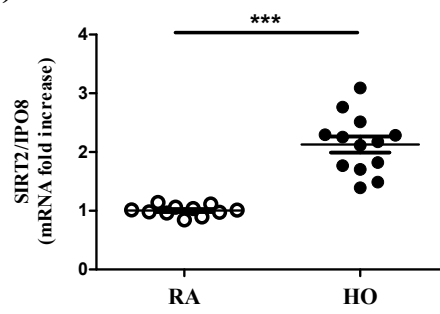
(SEM) of at least three independent experiments. Two-group comparisons were performed using a Student's *t*-test or a Mann-Whitney U test. For multiple group comparisons, one-way analysis of variance (ANOVA) or two-way ANOVA was used. The survival test was analyzed using the log-rank (Mantel-Cox) test. A *p*-value <0.05 was considered statistically significant.

## 3. Results

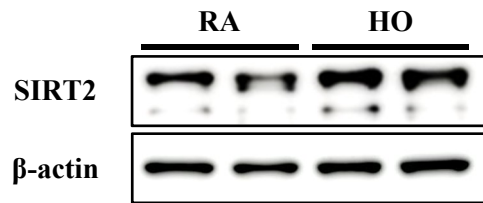
### 3.1. SIRT2 expression levels are increased by hyperoxia

To determine whether SIRT2 is involved in hyperoxia-induced acute lung injury, the expression levels of SIRT2 were examined in WT mice exposed to room air (RA) or hyperoxia (>95% O<sub>2</sub>; HO) for 72 hours. In WT mice exposed to hyperoxia, the mRNA expression levels of SIRT2 were observed to be higher than those in WT mice exposed to room air (Fig. 1A). Hyperoxic exposure also resulted in increased protein levels of SIRT2 in the lung lysates (Fig. 1B, C). Moreover, SIRT2-positive cells were elevated in the lung tissue of hyperoxia-exposed WT mice (Fig. 1D, E). These results suggest that SIRT2 is associated with hyperoxic acute lung injury.

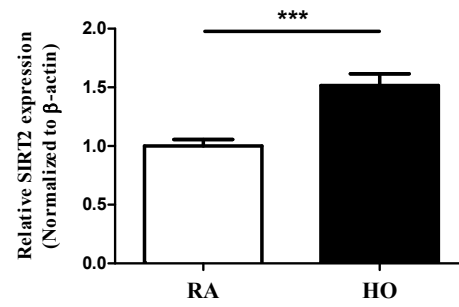
(A)



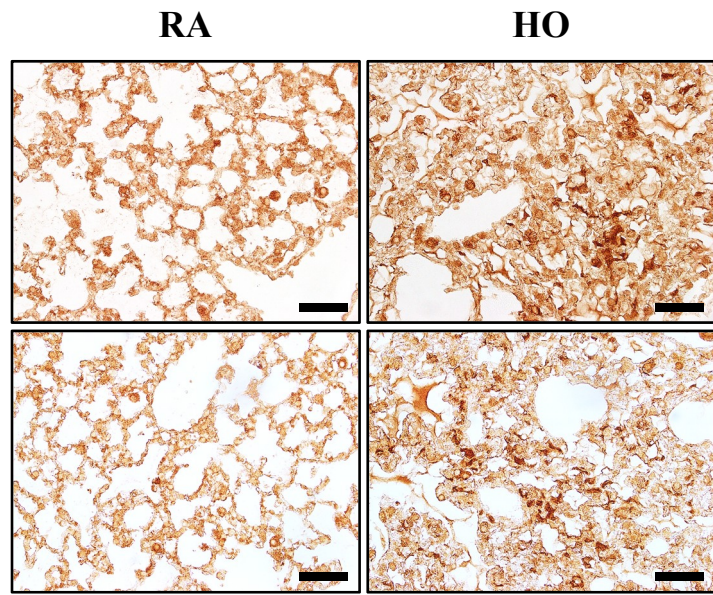
(B)



(C)



(D)



(E)

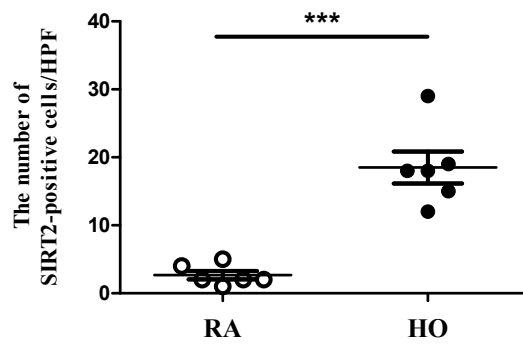
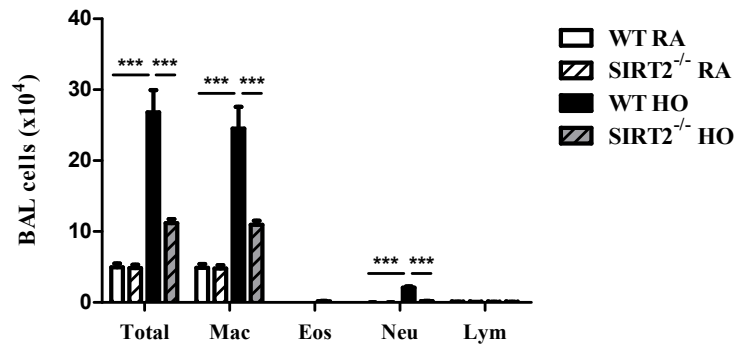


**Fig. 1. SIRT2 expression is elevated by hyperoxia.** Mice were exposed to room air or hyperoxia for 72 hours. (A) SIRT2 mRNA expression levels measured in lung tissues by real-time PCR. (B) The protein levels of SIRT2 in the lungs assessed by western blot and (C) the signal intensity quantified by densitometric analysis. (D) Representative immunohistochemistry images of SIRT2 staining in lung sections. (E) Graph showing the quantification of SIRT2-positive cells per HPF. Data represent the mean  $\pm$  SEM of at least three independent experiments (n = 11–13 mice per group). Scale bars in (D); 20  $\mu$ m. \*\*\* $P$  < 0.001. WT, wild-type; SIRT2, sirtuin 2; RA, room air; HO, hyperoxia; PCR, polymerase chain reaction; HPF, high-power field; SEM, standard error of the mean.

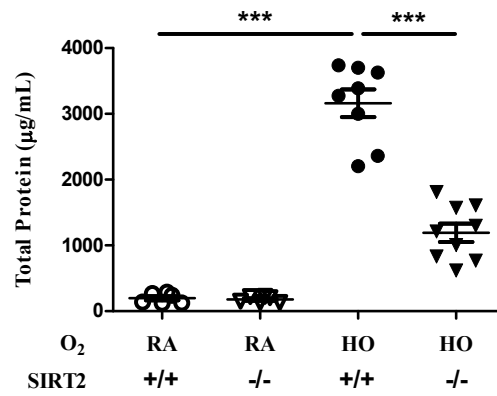
### 3.2. The absence of SIRT2 mitigates inflammation in hyperoxic acute lung injury

To investigate the contribution of SIRT2 in hyperoxia-induced pulmonary inflammation, WT and SIRT2<sup>-/-</sup> mice were treated with hyperoxia as described above to induce hyperoxic acute lung injury. After 72 hours of hyperoxic exposure, the number of total cells and inflammatory cells in BALF was increased in WT mice, whereas the numbers were comparatively decreased in SIRT2<sup>-/-</sup> mice (Fig. 2A). Total protein leakage in BALF was significantly reduced in SIRT2<sup>-/-</sup> mice exposed to hyperoxia compared to WT mice exposed to hyperoxia (Fig. 2B). Subsequently, the levels of pro-inflammatory cytokines, which play an important role in acute lung injury, were examined in WT mice and SIRT2<sup>-/-</sup> mice following hyperoxic exposure. In the hyperoxia group, IL-6, IL-1 $\beta$ , and TNF- $\alpha$  mRNA expression levels in the lungs were significantly lower in the absence of SIRT2 (Fig. 2C–E). Likewise, deficiency of SIRT2 led to diminished concentrations of IL-6, IL-1 $\beta$ , and TNF- $\alpha$  in BALF upon hyperoxic exposure (Fig. 2F–H). Additionally, hematoxylin and eosin staining were executed for histological analysis. Compared with WT mice kept in room air, exacerbated inflammatory cell infiltration and thickened alveolar walls were observed in lung tissue of WT mice exposed to hyperoxia. In contrast, lung inflammation was markedly alleviated in hyperoxia-exposed SIRT2<sup>-/-</sup> mice (Fig. 2I). Next, the mortality rates were compared between WT and SIRT2<sup>-/-</sup> mice through the survival test in which high oxygen was continuously administered. SIRT2<sup>-/-</sup> mice had a higher survival rate than WT mice under prolonged hyperoxic conditions (median survival = 87.5 hours in WT mice, and 97 hours in SIRT2<sup>-/-</sup> mice; Fig. 2J). These data demonstrated that the absence of SIRT2 lessens inflammation in hyperoxic acute lung injury.

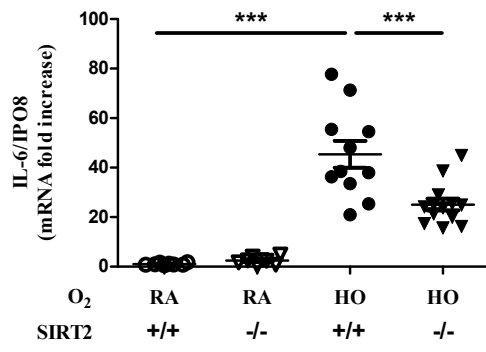
(A)



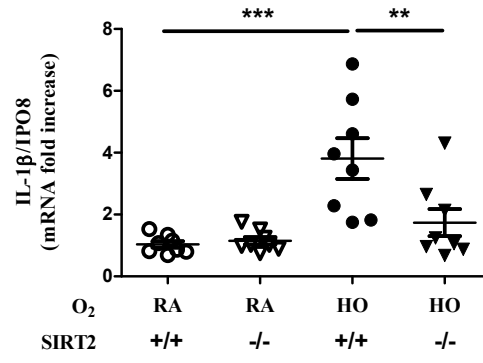
(B)



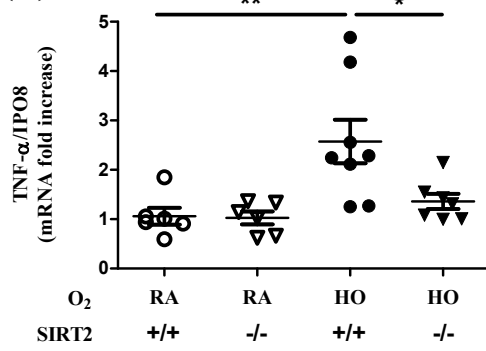
(C)



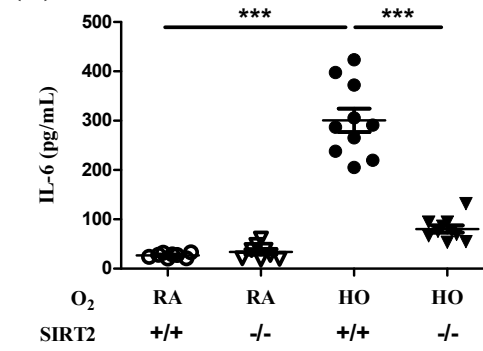
(D)



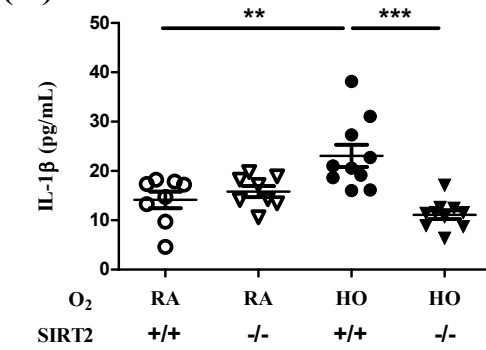
(E)



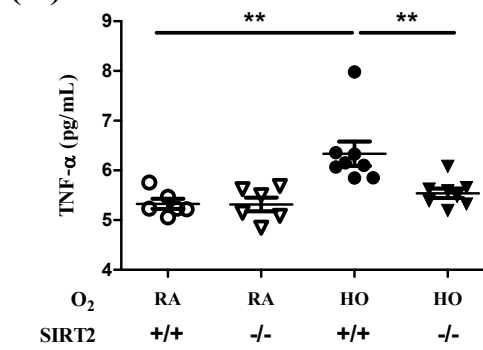
(F)



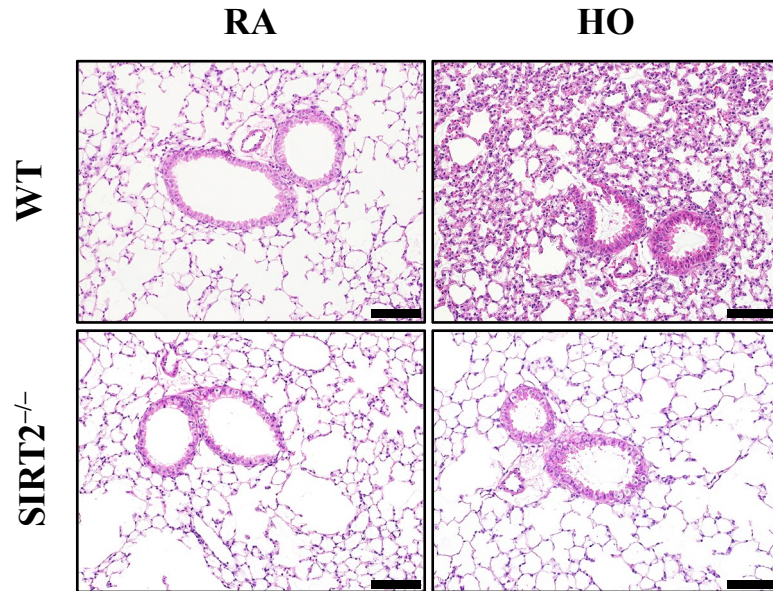
(G)



(H)



**(I)**



**(J)**

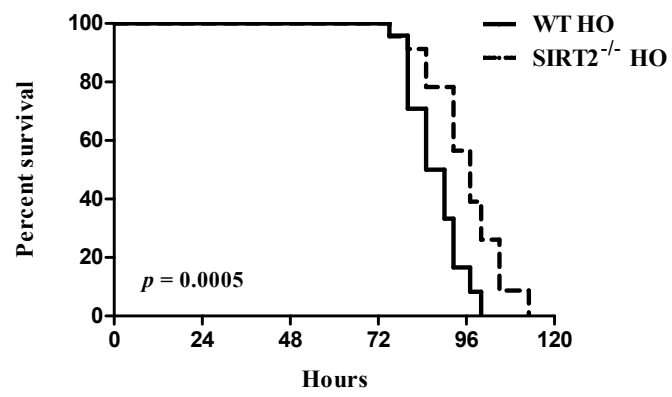
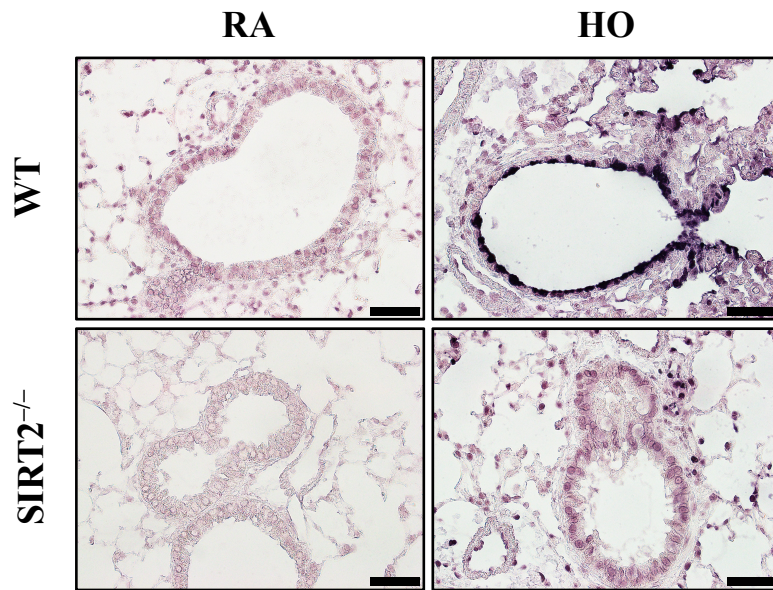


**Fig. 2. SIRT2 deficiency attenuates inflammation in hyperoxic acute lung injury.** WT and SIRT2<sup>-/-</sup> mice were exposed to RA or HO for 72 hours. (A) Total cells and inflammatory cells counted in BALF. (B) Total protein leakage of BALF assessed by BCA assay. (C–E) The mRNA expression levels of IL-6, IL-1 $\beta$ , and TNF- $\alpha$  in mouse lung tissues measured by real-time PCR. (F–H) Concentrations of IL-6, IL-1 $\beta$ , and TNF- $\alpha$  in BALF analyzed by ELISA. (I) Histological analysis of lung sections conducted through H&E staining. (J) Survival rates in WT and SIRT2<sup>-/-</sup> mice under hyperoxic conditions. Data represent the mean  $\pm$  SEM of at least three independent experiments (n = 6–13 mice per group). Scale bars in (I); 100  $\mu$ m. \**P* < 0.05, \*\**P* < 0.01, \*\*\**P* < 0.001. WT, wild-type; SIRT2, sirtuin 2; SIRT2<sup>-/-</sup>, SIRT2 deficient; RA, room air; HO, hyperoxia; BALF, bronchoalveolar lavage fluid; BCA, bicinchoninic acid; IL, interleukin; PCR, polymerase chain reaction; ELISA, enzyme-linked immunosorbent assay; H&E, hematoxylin and eosin; SEM, standard error of the mean.

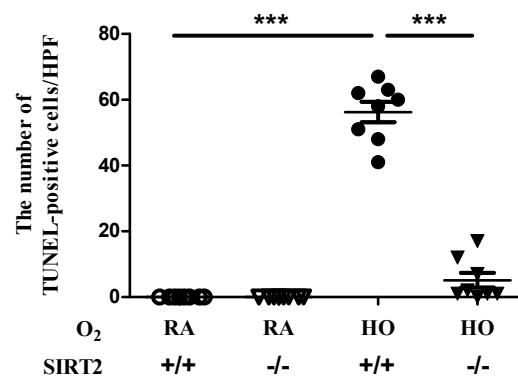
### 3.3. Deletion of SIRT2 leads to diminished apoptosis

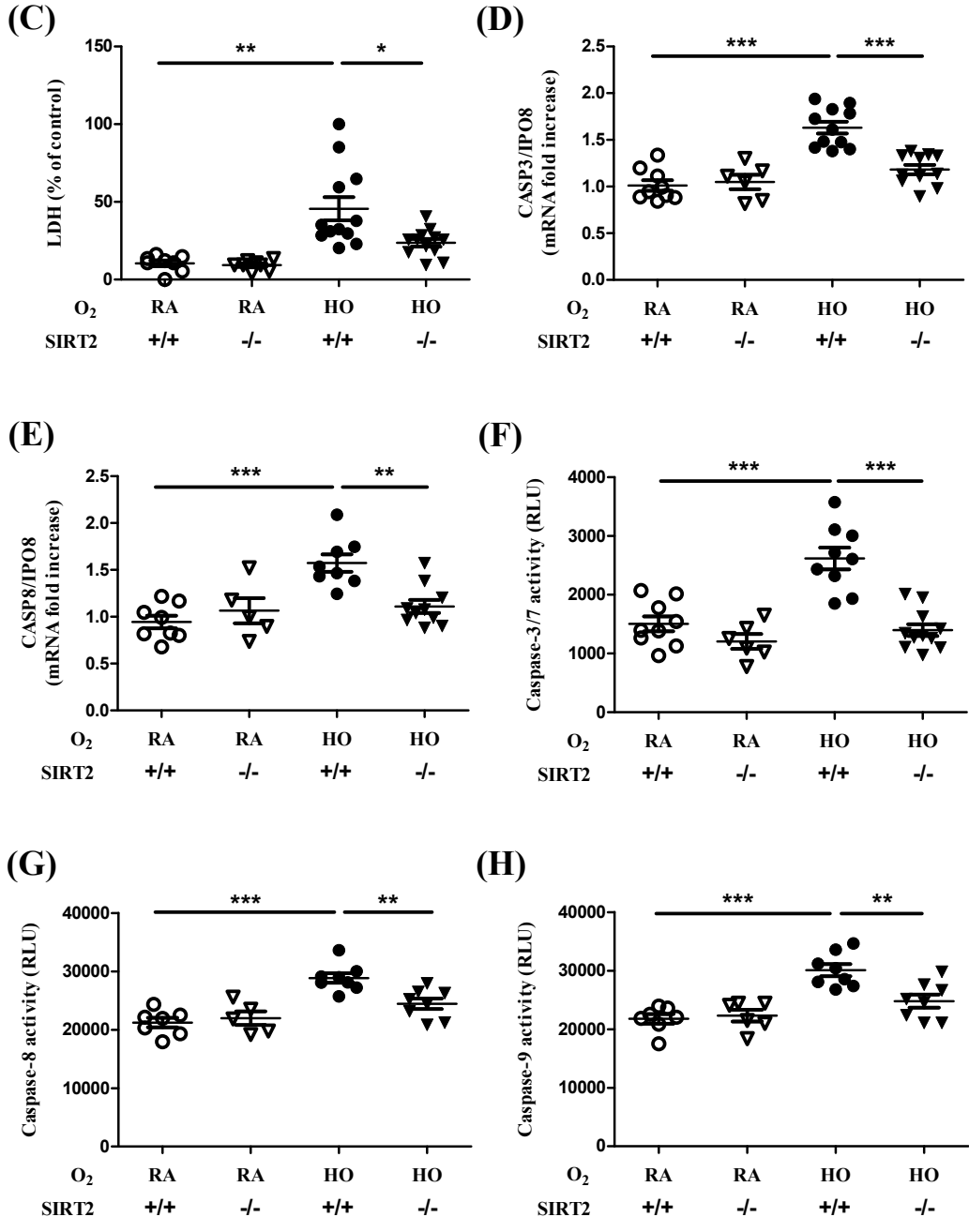
Since apoptosis is one of the representative pathological features of hyperoxia, apoptotic cells were analyzed by TUNEL assay to examine the impact of SIRT2 on hyperoxia-induced cell death. After hyperoxic exposure, apoptosis of lung alveolar cells was heightened in WT mice, but lessened in SIRT2<sup>-/-</sup> mice (Fig. 3A, B). Cell cytotoxicity in BALF was also dampened in hyperoxia-exposed SIRT2<sup>-/-</sup> mice compared to hyperoxia-exposed WT mice (Fig. 3C). To further ascertain the contribution of SIRT2 in hyperoxia-induced apoptosis, the mRNA expression levels and activities of caspases were assessed. Following hyperoxic exposure, the mRNA expression levels of caspase-3 and -8 in the lungs were increased in WT mice, but comparatively low in the absence of SIRT2 (Fig. 3D, E). Moreover, SIRT2 deficiency resulted in significantly lower activities of caspase-3/7, -8, and -9 in the lung lysates under hyperoxic conditions (Fig. 3F–H). Additionally, the expression of BAX and cytochrome C, which are important for initiating the apoptosis pathway, were examined using western blot analysis. Both BAX and cytochrome C expression levels were enhanced in WT mice exposed to hyperoxia, but significantly diminished in SIRT2<sup>-/-</sup> mice exposed to hyperoxia (Fig. 3I–K). These results suggest that SIRT2 mediates hyperoxia-induced apoptosis.

(A)



(B)





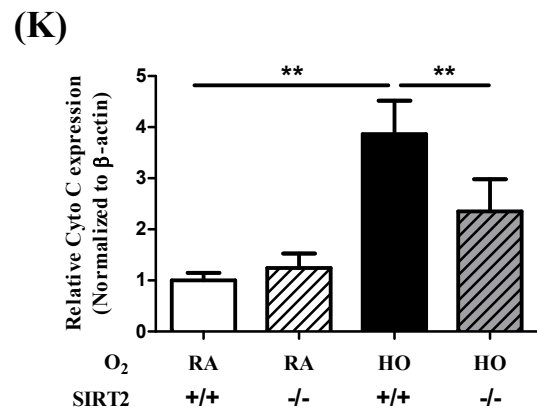
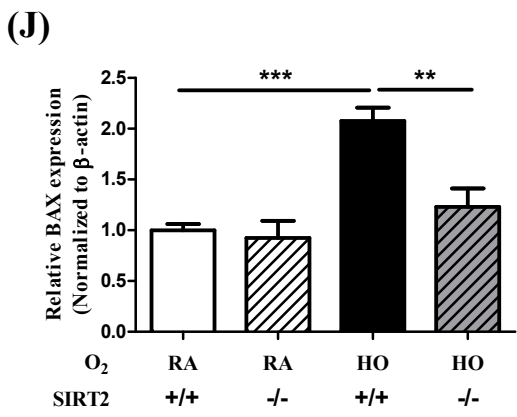
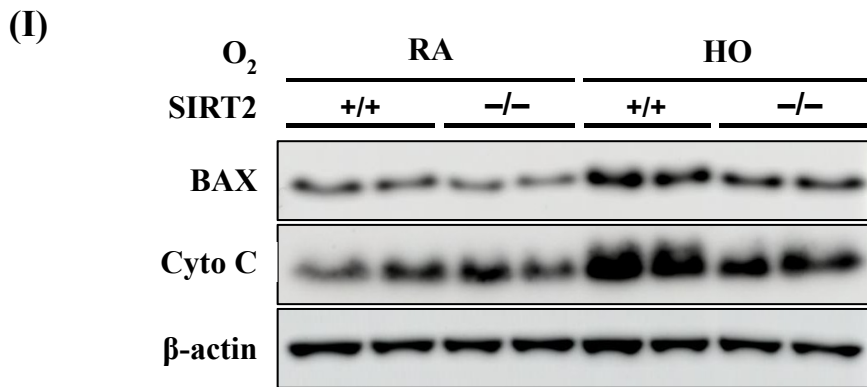
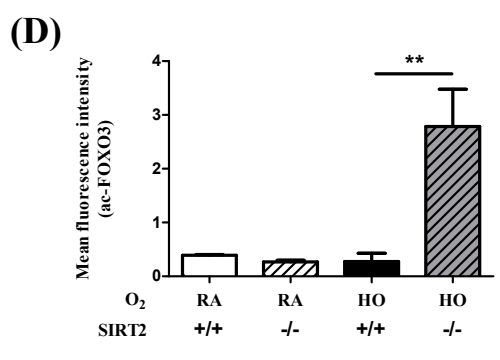
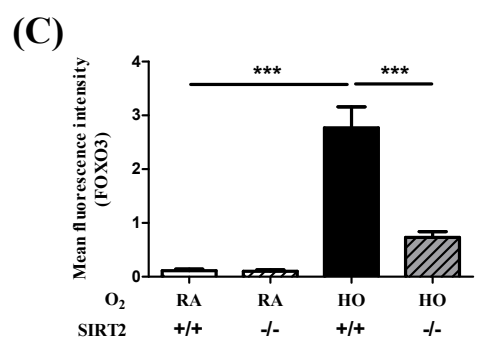
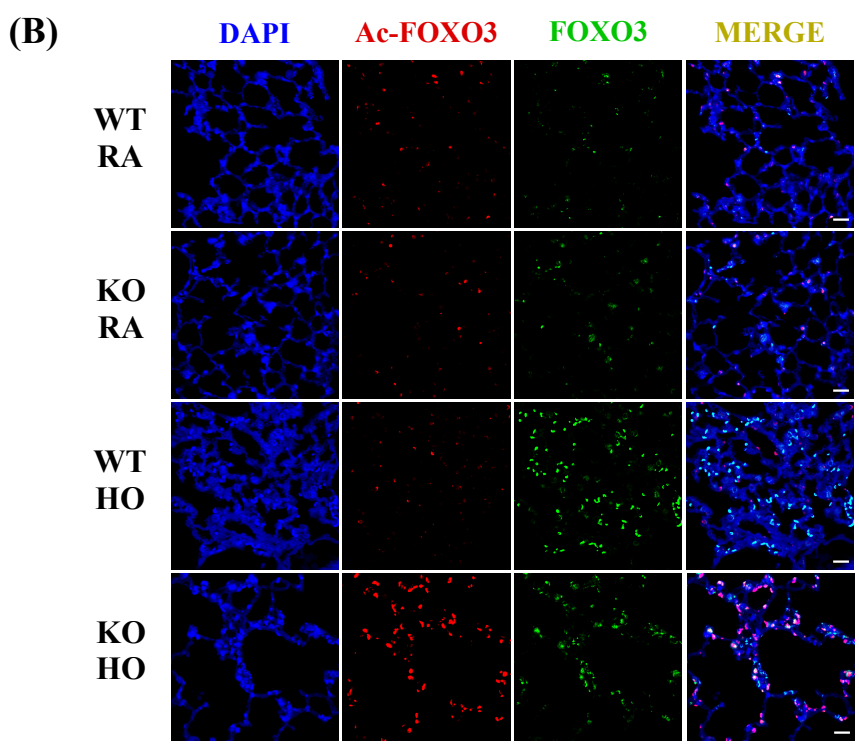
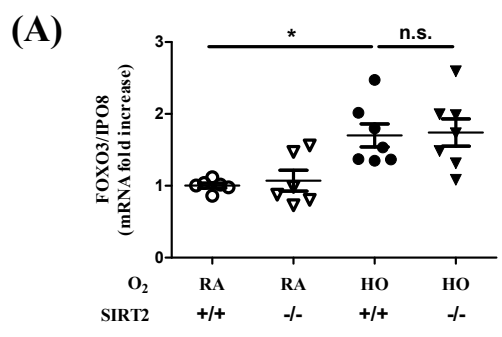


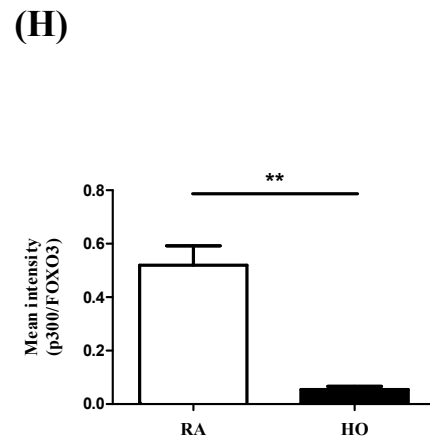
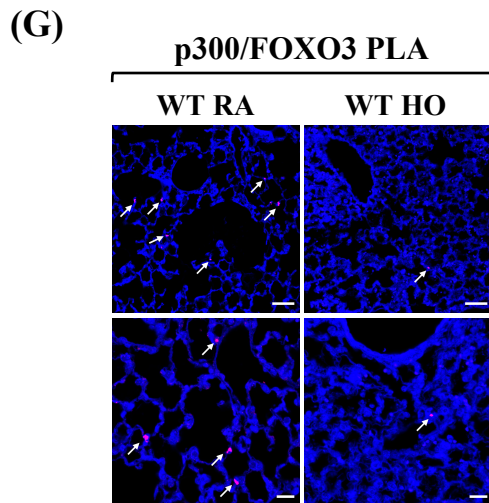
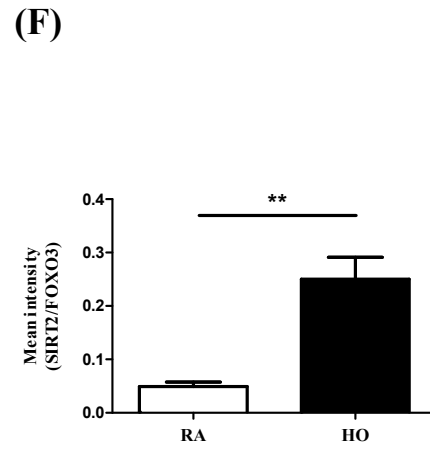
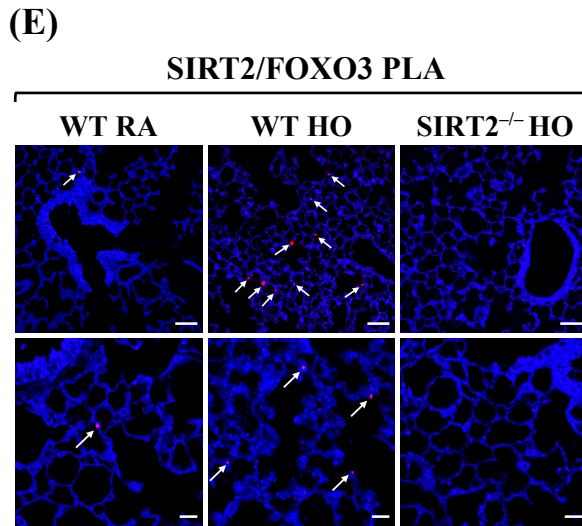
**Fig. 3. The absence of SIRT2 ameliorates apoptosis in hyperoxic acute lung injury.** (A) Representative images of TUNEL staining in mouse lung tissues. (B) Graph counted TUNEL-positive cells per HPF. (C) Cell cytotoxicity in BALF assessed by LDH assay. (D, E) The mRNA levels of CASP-3 and -8 in the lungs measured by real-time PCR. (F–H) Caspase-3/7, -8, and -9 activities detected in the lung lysates. (I) The protein levels of BAX and Cyto C in the lung lysates analyzed by western blot and (J, K) the signal intensity quantified by densitometric analysis. Data represent the mean  $\pm$  SEM of at least three independent experiments (n = 6–12 mice per group). Scale bars in (A); 20  $\mu$ m. \* $P$  < 0.05, \*\* $P$  < 0.01, \*\*\* $P$  < 0.001. WT, wild-type; SIRT2, sirtuin 2; SIRT2<sup>-/-</sup>, SIRT2 deficient; RA, room air; HO, hyperoxia; TUNEL, terminal deoxynucleotidyl transferase dUTP nick end labeling; HPF, high-power field; BALF, bronchoalveolar lavage fluid; CASP, caspase; PCR, polymerase chain reaction; Cyto C, cytochrome C; SEM, standard error of the mean.

### 3.4. SIRT2 regulates apoptosis by deacetylates FOXO3 in hyperoxic acute lung injury

SIRT2 is known to deacetylate FOXO3 in response to oxidative stress.<sup>30</sup> Therefore, this study next sought to determine whether SIRT2 affects FOXO3 in hyperoxia-induced acute lung injury. The mRNA expression levels of FOXO3 were higher in the hyperoxia group than those in the room air group, but there was no significant difference between the WT mice and SIRT2<sup>-/-</sup> mice in the hyperoxia group (Fig. 4A). For further investigation, the expression of FOXO3 and acetyl-FOXO3 in lung tissues were evaluated by immunofluorescence staining. In WT mice exposed to hyperoxia, the expression of FOXO3 was strikingly enhanced compared to WT mice exposed to room air. Additionally, the expression was comparatively weakened in the absence of SIRT2 upon hyperoxic exposure (Fig. 4B, C). However, surprisingly, contrary to the observed FOXO3 expression, the expression of acetyl-FOXO3 was dramatically increased in SIRT2 deficiency after hyperoxic exposure, indicating the regulation of FOXO3 deacetylation via SIRT2 (Fig. 4B, D). SIRT2 and p300 are known to be involved in the acetylation of FOXO3.<sup>27</sup> Therefore, the PLA assay was performed in lung tissues to visualize the interaction between SIRT2 and FOXO3, as well as between p300 and FOXO3. The PLA signals of SIRT2 and FOXO3 were only observed in WT mice, and it was augmented further upon exposure to hyperoxia (Fig. 4E, F). In contrast, PLA signals of p300 and FOXO3 were decreased after hyperoxia (Fig. 4G, H). Consequently, these outcomes indicate that SIRT2 deacetylates FOXO3 by interacting with it in hyperoxic acute lung injury.

Given that SIRT2 deacetylates FOXO3 in hyperoxic acute lung injury, the subsequent inquiry focused on whether SIRT2 affects target genes of FOXO3 related to apoptosis in hyperoxic acute lung injury. After hyperoxic exposure, the mRNA expression levels of the pro-apoptotic molecules BIM, PUMA, and PERP were upregulated, while a relative downregulation was observed when SIRT2 was deficient (Fig. 4I–K). Conversely, the mRNA expression levels of AATF, known to inhibit apoptosis, were significantly increased in the absence of SIRT2 after hyperoxic exposure (Fig. 4L). These findings demonstrate that SIRT2 mediates apoptosis signaling via FOXO3 deacetylation in hyperoxic acute lung injury.





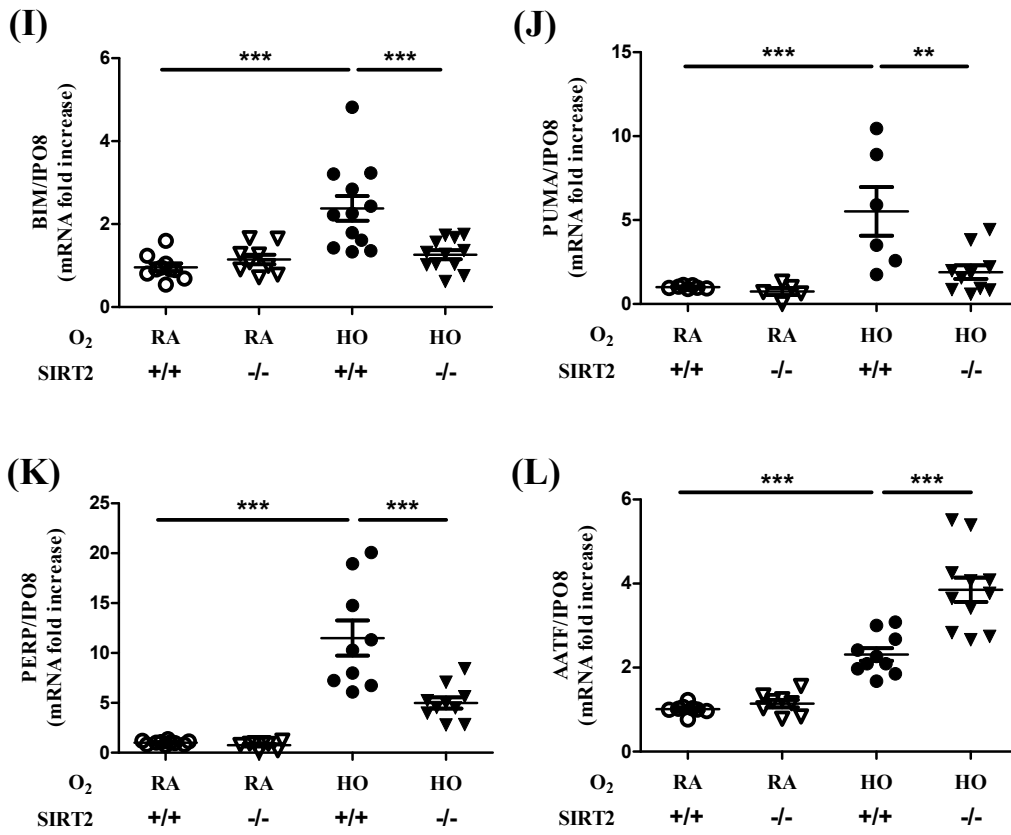
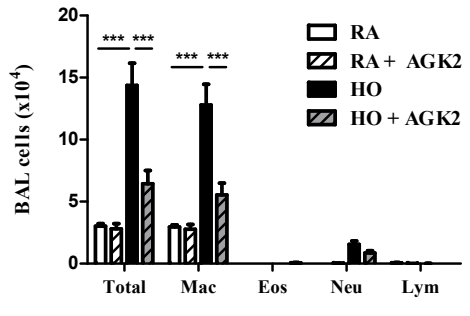


**Fig. 4. SIRT2 promotes apoptosis through deacetylating FOXO3.** (A) The mRNA expression levels of FOXO3 in lung tissues measured by real-time PCR. (B) Representative images of immunofluorescence staining for FOXO3 and acetyl-FOXO3 in lung sections. (C) The mean intensity of FOXO3. (D) The mean intensity of ac-FOXO3. (E) PLA images for SIRT2 and FOXO3 in lung samples. (F) The mean intensity of PLA signals for SIRT2 and FOXO3. (G) PLA images for p300 and FOXO3 in lung samples. (H) The mean intensity of PLA signals for p300 and FOXO3. (I–L) BIM, PUMA, PERP, and AATF mRNA expression levels in the lungs analyzed by real-time PCR. Data represent the mean  $\pm$  SEM of at least three independent experiments (n = 5–12 mice per group). Scale bars in (B); 20  $\mu$ m. Scale bars in (E) and (G); 50  $\mu$ m (top) and 20  $\mu$ m (bottom). \* $P$  < 0.05, \*\* $P$  < 0.01, \*\*\* $P$  < 0.001. WT, wild-type; SIRT2, sirtuin 2; SIRT2<sup>-/-</sup>, SIRT2 deficient; RA, room air; HO, hyperoxia; FOXO3, forkhead box O3; Ac-FOXO3, acetyl-FOXO3; PLA, proximity ligation assay; BIM, Bcl-2-like protein 11; PUMA, p53 upregulated modulator of apoptosis; PERP, TP53 apoptosis effector; AATF, apoptosis antagonizing transcription factor; PCR, polymerase chain reaction; SEM, standard error of the mean.

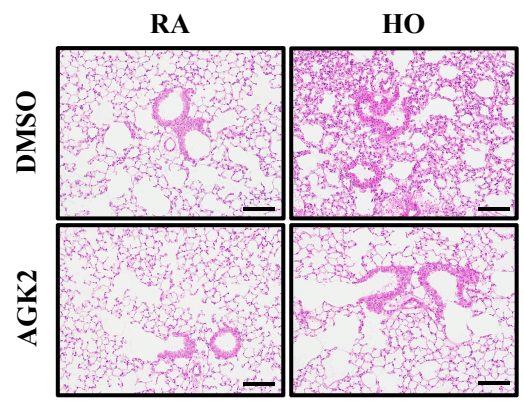
### 3.5. Inhibition of SIRT2 ameliorates hyperoxic acute lung injury

Lastly, to identify whether SIRT2 can be used as a therapeutic target in hyperoxic acute lung injury, AGK2, an inhibitor of SIRT2, was administered to mice and then evaluated. After hyperoxic exposure, the total and inflammatory cell counts in BALF were decreased in AGK2-treated mice compared to control mice (Fig. 5A). In hematoxylin & eosin staining of lung tissues, the administration of AGK2 has been shown to alleviate the extent of lung injury caused by hyperoxia (Fig. 5B). Moreover, IL-6 and IL-1 $\beta$  concentrations in BALF were significantly lessened upon treatment of AGK2 following hyperoxic exposure (Fig. 5C, D). Additionally, TUNEL assay was performed to investigate the impact of AGK2 treatment on hyperoxia-induced apoptosis. In lung tissues, the administration of AGK2 was found to reduce the number of apoptotic cells due to hyperoxia (Fig. 5E). Furthermore, caspase-3/7 activity was also diminished by AGK2 treatment (Fig. 5F). Therefore, these data indicate that the inhibition of SIRT2 via AGK2 treatment had a therapeutic effect in mitigating hyperoxia-induced lung injury.

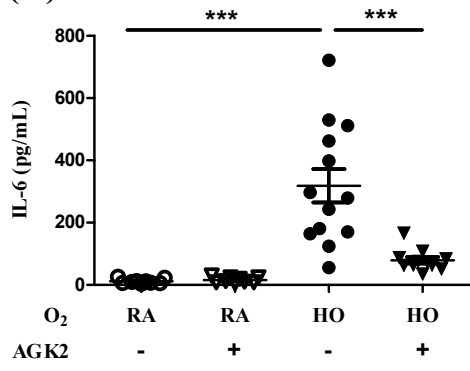
(A)



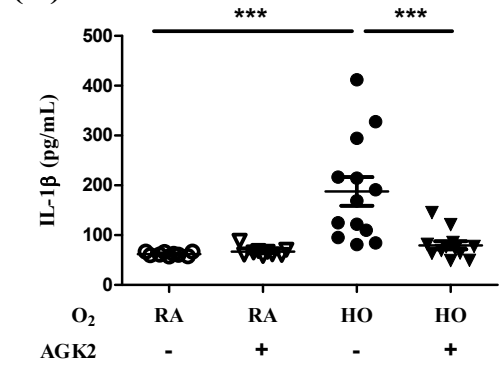
(B)



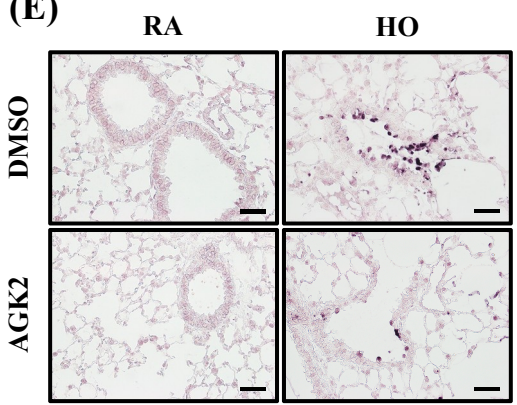
(C)



(D)



(E)



(F)

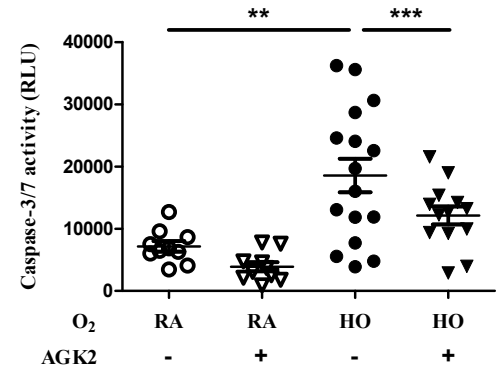


**Fig. 5. AGK2 improves hyperoxic acute lung injury.** AGK2 or DMSO was administered to mice by intraperitoneal injection before hyperoxic exposure. (A) Total cells and inflammatory cells counted in BALF. (B) Histological analysis of lung tissues performed through H&E staining. (C, D) IL-6 and IL-1 $\beta$  concentrations in BALF measured by ELISA. (E) Representative images of TUNEL staining in lung sections. (F) Caspase-3/7 activity analyzed in the lung lysates. Data represent the mean  $\pm$  SEM of at least three independent experiments (n = 6–16 mice per group). Scale bars in (B); 50  $\mu$ m. Scale bars in (E); 20  $\mu$ m. \*\* $P$  < 0.01, \*\*\* $P$  < 0.001. SIRT2, sirtuin 2; BALF, bronchoalveolar lavage fluid; TUNEL, terminal deoxynucleotidyl transferase dUTP nick end labeling; DMSO, dimethyl sulfoxide; H&E, hematoxylin and eosin; ELISA, enzyme-linked immunosorbent assay; SEM, standard error of the mean.

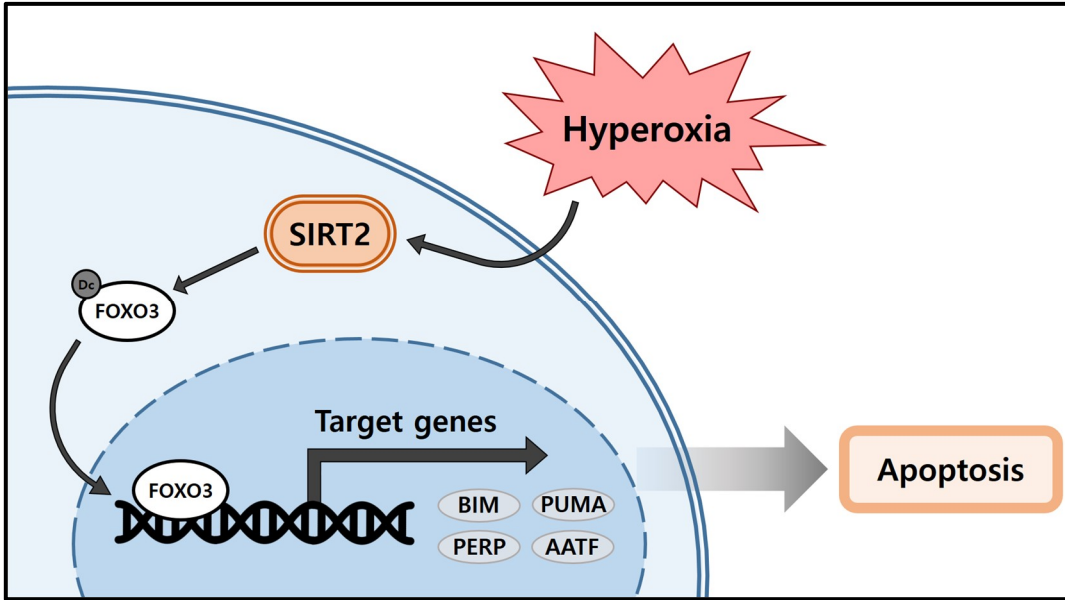


**Fig. 6. SIRT2 mediates FOXO3 deacetylation to promote transcriptional activation of FOXO3 target genes related to apoptosis in hyperoxic acute lung injury.** SIRT2 expression levels were significantly increased after hyperoxic exposure. SIRT2 interacted with FOXO3 to directly deacetylate it under hyperoxic conditions. SIRT2 regulates the expression levels of FOXO3 target genes associated with apoptosis by deacetylating FOXO3 in hyperoxic acute lung injury.

## 4. Discussion

This study found that SIRT2 expression increases during hyperoxic exposure, leading to enhanced lung damage and inflammatory responses. The current research also demonstrates that SIRT2 regulates hyperoxia-mediated apoptosis signaling through deacetylation of FOXO3 in the pathogenesis of hyperoxic acute lung injury. Furthermore, the present study addresses that the administration of a SIRT2 inhibitor results in attenuated pathogenesis in hyperoxic acute lung injury.

SIRT2, one of the most underexplored members of the sirtuin family, has been increasingly reported to play multiple roles in a wide range of diseases and physiological processes.<sup>19</sup> SIRT2 is expressed in a variety of tissues and organs, contributing to metabolic processes, inflammatory responses, and oxidative stress.<sup>31</sup> Additionally, SIRT2 has been confirmed to be implicated in diverse diseases including cancer, type 2 diabetes, colitis, arthritis, and neurological disorders, although its role in certain diseases remains controversial.<sup>22,23,31-33</sup> Several cancer-related studies have shown that SIRT2 has a role in tumorigenesis, with both tumor-promoting and tumor-suppressing function.<sup>21</sup> The present study indicated that the absence of SIRT2 alleviates hyperoxic acute lung injury. Consistent with the findings of this study, recent studies have demonstrated that inhibiting SIRT2 reduced the pathogenesis of asthma and lung fibrosis.<sup>34,35</sup> Another study also noted that cisplatin-induced acute kidney injury was reduced in SIRT2 deficiency.<sup>36</sup> Similarly, inhibiting SIRT2 has been observed to suppress inflammatory responses and apoptosis in thioacetamide-induced acute liver failure.<sup>37</sup> Comprehensively, these results manifest that SIRT2 plays as an important regulator in various pathogenic mechanisms, including lung diseases and acute lesions.

Hyperoxia induces lung damage characterized by diffuse infiltration of diverse inflammatory cells, heightened pulmonary permeability, and compromised alveolar development.<sup>38,39</sup> In this study, exposure to hyperoxia increased pulmonary inflammation and expression of pro-inflammatory cytokines, while it was lessened in the absence of SIRT2. The primary molecular mechanism of this hyperoxia-induced lung injury is known as apoptosis, accompanying the activation of caspase cascade and components of the extrinsic and intrinsic cell death pathways.<sup>40</sup> In the series of apoptosis processes, the BH3-only proteins, such as BIM, PUMA

and BID, activate the pro-apoptotic effector proteins BAX and BAK, leading to the release of cytochrome C, which in turn promotes the activation of caspases.<sup>41</sup> According to *in vitro* studies using PC12 cells and HeLa cells, SIRT2 knockdown attenuated apoptosis under H<sub>2</sub>O<sub>2</sub>-induced oxidative stress.<sup>42,43</sup> In line with the previous studies, the current study also observed that the expression of BAX and cytochrome C as well as the activities of caspase-3/7, -8, and -9 were significantly lower in SIRT2<sup>-/-</sup> mice compared to WT mice under hyperoxic conditions.

FOXO3, one of the major targets of SIRT2 is known to mediate various cellular processes by inducing the transcription of target genes associated with apoptosis, proliferation, DNA damage, survival, and cell cycle progression.<sup>26</sup> Various PTMs regulate the activity of FOXO3 by altering its subcellular localization and DNA-binding activity.<sup>44</sup> The results of immunofluorescence staining in lung tissues showed that FOXO3 expression was increased in both WT mice and SIRT2<sup>-/-</sup> mice upon hyperoxic exposure, while acetyl-FOXO3 expression was surprisingly heightened in hyperoxia-exposed SIRT2<sup>-/-</sup> mice. Furthermore, the increase in PLA signals for SIRT2 and FOXO3 upon hyperoxic exposure showed that SIRT2 directly deacetylates FOXO3, thereby reducing the expression of acetyl-FOXO3. Overall, these results indicate that the absence of SIRT2 leads to changes in FOXO3 deacetylation, resulting in more abundant FOXO3 acetylation. Additionally, the interaction between p300 and FOXO3 was investigated, since p300 is one of the molecules known to acetylate FOXO3. Contrary to the results of the PLA signals for SIRT2 and FOXO3, it is noteworthy that the interaction between p300 and FOXO3 is reduced by hyperoxia. These data support that SIRT2 mediates deacetylation of FOXO3 in hyperoxic acute lung injury.

In contrast to the deacetylation of other nucleosomal histones, the transcriptional activation of FOXO3 has been shown to be enhanced through deacetylation.<sup>27,29</sup> SIRT2 deacetylates FOXO3 to promote nuclear localization, and activated FOXO3 binds to the DNA binding domain to enhance transcription of target genes.<sup>27,44</sup> Likewise, as shown in Fig. 4B, this data demonstrates that FOXO3 expressed in hyperoxia-exposed WT mice was condensed in the nucleus, whereas FOXO3 expressed in hyperoxia-exposed SIRT2<sup>-/-</sup> mice was spread throughout. Previous studies have shown that BIM and PUMA, which belong to BH3-only proteins of Bcl-2 family, are upregulated by FOXO3.<sup>30,45</sup> In addition, PERP and AATF were identified as target genes of FOXO3 related to apoptosis through the Harmonizome 3.0 database.<sup>46</sup> PERP (p53 apoptosis effector related to PMP-22) is known to facilitate pro-

apoptotic function across various cell types and tissues, and AATF (apoptosis antagonizing transcription factor) is known to promote cell survival by suppressing apoptosis.<sup>47,48</sup> Astonishingly, this study showed that hyperoxic exposure led to an upregulation of apoptosis-promoting genes BIM, PUMA, and PERP, whereas a comparative downregulation was observed in the deficiency of SIRT2. However, AATF expression levels were elevated in SIRT2<sup>-/-</sup> mice compared to WT mice. Hence, these results indicate that SIRT2 is engaged in apoptotic signaling by modulating the transcription of FOXO3 target genes through FOXO3 deacetylation.

Several studies have documented that SIRT2 inhibitor AGK2 attenuated fibrosis and inflammation.<sup>34,49</sup> In the present study, treatment of AGK2 alleviated hyperoxia-induced inflammation and apoptosis, consistent with the results using SIRT2<sup>-/-</sup> mice. These results showed that AGK2 treatment has a therapeutic effect on hyperoxic acute lung injury. Overall, this study suggests that SIRT2 may be a new therapeutic target for hyperoxic acute lung injury.

## 5. Conclusion

In the present study, it was revealed that SIRT2 expression was significantly increased in hyperoxia-induced acute lung injury. Within the hyperoxia group, SIRT2<sup>-/-</sup> mice displayed alleviation of the lung inflammation, and exhibited a higher survival rate under continual hyperoxic conditions compared to WT mice. Further investigation demonstrated that hyperoxia-induced apoptosis was mitigated in SIRT2<sup>-/-</sup> mice when compared to WT mice. Decisively, SIRT2 interacted with FOXO3 to directly deacetylate it, thereby regulating the expression levels of FOXO3 target genes associated with apoptosis. Moreover, in SIRT2 inhibitor study, pharmacological inhibition of SIRT2 attenuated hyperoxia-induced inflammation and apoptosis. Taken together, this study suggests that SIRT2 plays a crucial role in the pathogenesis of hyperoxic acute lung injury by deacetylating FOXO3 to regulate apoptosis signaling.

## References

1. Kallet RH, Matthay MA. Hyperoxic acute lung injury. *Respir Care* 2013;58:123-41.
2. Amarelle L, Quintela L, Hurtado J, Malacrida L. Hyperoxia and Lungs: What We Have Learned From Animal Models. *Front Med (Lausanne)* 2021;8:606678.
3. Sidramagowda Patil S, Hernández-Cuervo H, Fukumoto J, Krishnamurthy S, Lin M, Alleyn M, et al. Alda-1 Attenuates Hyperoxia-Induced Acute Lung Injury in Mice. *Front Pharmacol* 2020;11:597942.
4. Grimm SL, Stading RE, Robertson MJ, Gandhi T, Fu C, Jiang W, et al. Loss of cytochrome P450 (CYP)1B1 mitigates hyperoxia response in adult mouse lung by reprogramming metabolism and translation. *Redox Biol* 2023;64:102790.
5. Sohn MH, Kang MJ, Matsuura H, Bhandari V, Chen NY, Lee CG, et al. The chitinase-like proteins breast regression protein-39 and YKL-40 regulate hyperoxia-induced acute lung injury. *Am J Respir Crit Care Med* 2010;182:918-28.
6. Lilien TA, van Meenen DMP, Schultz MJ, Bos LDJ, Bem RA. Hyperoxia-induced lung injury in acute respiratory distress syndrome: what is its relative impact? *Am J Physiol Lung Cell Mol Physiol* 2023;325:L9-116.
7. Ren Y, Qin S, Liu X, Feng B, Liu J, Zhang J, et al. Hyperoxia can Induce Lung Injury by Upregulating AECII Autophagy and Apoptosis Via the mTOR Pathway. *Mol Biotechnol* 2023; doi:10.1007/s12033-023-00945-2.
8. Mach WJ, Thimmesch AR, Pierce JT, Pierce JD. Consequences of hyperoxia and the toxicity of oxygen in the lung. *Nurs Res Pract* 2011;2011:260482.
9. Lius EE, Syafaah I. Hyperoxia in the management of respiratory failure: A literature review. *Ann Med Surg (Lond)* 2022;81:104393.
10. Hong JY, Kim MN, Kim EG, Lee JW, Kim HR, Kim SY, et al. Clusterin Deficiency Exacerbates Hyperoxia-Induced Acute Lung Injury. *Cells* 2021;10.
11. Kim HR, Kim MN, Kim EG, Leem JS, Baek SM, Lee YJ, et al. NLRX1 knockdown attenuates pro-apoptotic signaling and cell death in pulmonary hyperoxic acute injury. *Sci Rep* 2023;13:3441.
12. Gore A, Muralidhar M, Espey MG, Degenhardt K, Mantell LL. Hyperoxia sensing: from molecular mechanisms to significance in disease. *J Immunotoxicol* 2010;7:239-54.

13. Coarfa C, Grimm SL, Katz T, Zhang Y, Jangid RK, Walker CL, et al. Epigenetic response to hyperoxia in the neonatal lung is sexually dimorphic. *Redox Biol* 2020;37:101718.
14. Chen CM, Liu YC, Chen YJ, Chou HC. Genome-Wide Analysis of DNA Methylation in Hyperoxia-Exposed Newborn Rat Lung. *Lung* 2017;195:661-9.
15. Bik-Multanowski M, Revhaug C, Grabowska A, Dobosz A, Madetko-Talowska A, Zasada M, et al. Hyperoxia induces epigenetic changes in newborn mice lungs. *Free Radic Biol Med* 2018;121:51-6.
16. Zhu Y, Fu J, Yang H, Pan Y, Yao L, Xue X. Hyperoxia-induced methylation decreases RUNX3 in a newborn rat model of bronchopulmonary dysplasia. *Respir Res* 2015;16:75.
17. Portela A, Esteller M. Epigenetic modifications and human disease. *Nature Biotechnology* 2010;28:1057-68.
18. Zheng M, Hu C, Wu M, Chin YE. Emerging role of SIRT2 in non-small cell lung cancer. *Oncol Lett* 2021;22:731.
19. Wang Y, Yang J, Hong T, Chen X, Cui L. SIRT2: Controversy and multiple roles in disease and physiology. *Ageing Res Rev* 2019;55:100961.
20. North BJ, Verdin E. Interphase nucleo-cytoplasmic shuttling and localization of SIRT2 during mitosis. *PLoS One* 2007;2:e784.
21. Chen G, Huang P, Hu C. The role of SIRT2 in cancer: A novel therapeutic target. *Int J Cancer* 2020;147:3297-304.
22. Chen X, Lu W, Wu D. Sirtuin 2 (SIRT2): Confusing Roles in the Pathophysiology of Neurological Disorders. *Front Neurosci* 2021;15:614107.
23. Kitada M, Ogura Y, Monno I, Koya D. Sirtuins and Type 2 Diabetes: Role in Inflammation, Oxidative Stress, and Mitochondrial Function. *Front Endocrinol (Lausanne)* 2019;10:187.
24. Manjula R, Anuja K, Alcain FJ. SIRT1 and SIRT2 Activity Control in Neurodegenerative Diseases. *Front Pharmacol* 2020;11:585821.
25. Al-Tamari HM, Dabral S, Schmall A, Sarvari P, Ruppert C, Paik J, et al. FoxO3 an important player in fibrogenesis and therapeutic target for idiopathic pulmonary fibrosis. *EMBO Mol Med* 2018;10:276-93.
26. Liu Y, Ao X, Ding W, Ponnusamy M, Wu W, Hao X, et al. Critical role of FOXO3a in carcinogenesis. *Mol Cancer* 2018;17:104.
27. Wang X, Hu S, Liu L. Phosphorylation and acetylation modifications of FOXO3a:

- Independently or synergistically? *Oncol Lett* 2017;13:2867-72.
28. Wang Y, Mu Y, Zhou X, Ji H, Gao X, Cai WW, et al. SIRT2-mediated FOXO3a deacetylation drives its nuclear translocation triggering FasL-induced cell apoptosis during renal ischemia reperfusion. *Apoptosis* 2017;22:519-30.
  29. Wang Z, Yu T, Huang P. Post-translational modifications of FOXO family proteins (Review). *Mol Med Rep* 2016;14:4931-41.
  30. Wang F, Nguyen M, Qin FX, Tong Q. SIRT2 deacetylates FOXO3a in response to oxidative stress and caloric restriction. *Aging Cell* 2007;6:505-14.
  31. Zhu C, Dong X, Wang X, Zheng Y, Qiu J, Peng Y, et al. Multiple Roles of SIRT2 in Regulating Physiological and Pathological Signal Transduction. *Genet Res (Camb)* 2022;2022:9282484.
  32. Watanabe H, Inaba Y, Kimura K, Matsumoto M, Kaneko S, Kasuga M, et al. Sirt2 facilitates hepatic glucose uptake by deacetylating glucokinase regulatory protein. *Nature Communications* 2018;9:30.
  33. Lo Sasso G, Menzies KJ, Mottis A, Piersigilli A, Perino A, Yamamoto H, et al. SIRT2 deficiency modulates macrophage polarization and susceptibility to experimental colitis. *PLoS One* 2014;9:e103573.
  34. Gong H, Zheng C, Lyu X, Dong L, Tan S, Zhang X. Inhibition of Sirt2 Alleviates Fibroblasts Activation and Pulmonary Fibrosis via Smad2/3 Pathway. *Front Pharmacol* 2021;12:756131.
  35. Lee YG, Reader BF, Herman D, Streicher A, Englert JA, Ziegler M, et al. Sirtuin 2 enhances allergic asthmatic inflammation. *JCI Insight* 2019;4.
  36. Jung YJ, Park W, Kang KP, Kim W. SIRT2 is involved in cisplatin-induced acute kidney injury through regulation of mitogen-activated protein kinase phosphatase-1. *Nephrol Dial Transplant* 2020;35:1145-56.
  37. Jiao FZ, Wang Y, Zhang WB, Zhang HY, Chen Q, Shi CX, et al. Protective role of AGK2 on thioacetamide-induced acute liver failure in mice. *Life Sci* 2019;230:68-75.
  38. Obst S, Herz J, Alejandre Alcazar MA, Endesfelder S, Möbius MA, Rüdiger M, et al. Perinatal Hyperoxia and Developmental Consequences on the Lung-Brain Axis. *Oxidative Medicine and Cellular Longevity* 2022;2022:5784146.
  39. Alam MA, Betal SGN, Aghai ZH, Bhandari V. Hyperoxia causes miR199a-5p-mediated

- injury in the developing lung. *Pediatr Res* 2019;86:579-88.
40. Bhandari V, Elias JA. Cytokines in tolerance to hyperoxia-induced injury in the developing and adult lung. *Free Radic Biol Med* 2006;41:4-18.
  41. Czabotar PE, Lessene G, Strasser A, Adams JM. Control of apoptosis by the BCL-2 protein family: implications for physiology and therapy. *Nat Rev Mol Cell Biol* 2014;15:49-63.
  42. Nie H, Hong Y, Lu X, Zhang J, Chen H, Li Y, et al. SIRT2 mediates oxidative stress-induced apoptosis of differentiated PC12 cells. *Neuroreport* 2014;25:838-42.
  43. Sarikhani M, Mishra S, Desingu PA, Kotyada C, Wolfgeher D, Gupta MP, et al. SIRT2 regulates oxidative stress-induced cell death through deacetylation of c-Jun NH(2)-terminal kinase. *Cell Death Differ* 2018;25:1638-56.
  44. Orea-Soufi A, Paik J, Bragança J, Donlon TA, Willcox BJ, Link W. FOXO transcription factors as therapeutic targets in human diseases. *Trends Pharmacol Sci* 2022;43:1070-84.
  45. You H, Pellegrini M, Tsuchihara K, Yamamoto K, Hacker G, Erlacher M, et al. FOXO3a-dependent regulation of Puma in response to cytokine/growth factor withdrawal. *J Exp Med* 2006;203:1657-63.
  46. Rouillard AD, Gunderson GW, Fernandez NF, Wang Z, Monteiro CD, McDermott MG, et al. The harmonizome: a collection of processed datasets gathered to serve and mine knowledge about genes and proteins. *Database (Oxford)* 2016;2016.
  47. Davies L, Spiller D, White MR, Grierson I, Paraoan L. PERP expression stabilizes active p53 via modulation of p53-MDM2 interaction in uveal melanoma cells. *Cell Death Dis* 2011;2:e136.
  48. Srinivas AN, Suresh D, Mirshahi F, Santhekadur PK, Sanyal AJ, Kumar DP. Emerging roles of AATF: Checkpoint signaling and beyond. *J Cell Physiol* 2021;236:3383-95.
  49. Zhao T, Alam HB, Liu B, Bronson RT, Nikolian VC, Wu E, et al. Selective Inhibition of SIRT2 Improves Outcomes in a Lethal Septic Model. *Curr Mol Med* 2015;15:634-41.

## Abstract in Korean

### 고농도 산소 노출로 인한 급성 폐 손상 기전에서 SIRT2의 역할

**배경** : 산소 요법은 호흡이 어려운 환자에게 도움이 되지만, 고농도 산소를 지속적으로 투여받을 경우 고농도 산소로 인한 급성 폐 손상을 초래할 수 있다. Sirtuin 2 (SIRT2)는 nicotinamide adenine dinucleotide (NAD<sup>+</sup>)에 의존적인 탈아세틸화 효소로서, 폐섬유증, 세포사멸 및 염증에 관여하는 것으로 나타났다. 하지만, 고농도 산소로 인한 급성 폐 손상의 발병기전에서 SIRT2의 역할은 밝혀지지 않았다. 본 연구에서는 고농도 산소로 인한 급성 폐 손상에서 SIRT2의 역할을 밝히는 것을 목표로 하였다.

**방법** : 야생형 마우스와 SIRT2 결핍 마우스를 정상 산소 혹은 고농도 산소에 72시간 동안 노출시켰다. 그 다음 야생형 마우스와 SIRT2 결핍 마우스 사이의 고농도 산소로 인한 염증과 세포 사멸의 변화를 평가하였다. 그 다음, SIRT2 결핍 마우스에서 고농도 산소로 인한 급성 폐 손상의 변화에 forkhead box O3 (FOXO3)가 관여하는지 조사하였다. 추가적으로, SIRT2 억제제 연구를 통해 AGK2를 처리하였을 때 고농도 산소로 인한 염증 및 세포 사멸 정도를 평가하였다.

**결과** : 고농도 산소 노출 후 야생형 마우스에서 SIRT2의 발현이 현저히 증가하였다. 지속적인 고농도 산소 조건에서 SIRT2 결핍 마우스는 야생형 마우스보다 생존 기간이 길었다. 또한, 기관지 폐포 세척액의 총 세포 수, 전염증성 사이토카인 발현 및 조직학적 폐 손상은 고농도 산소에 노출된 야생형 마우스에 비해 고농도 산소에 노출된 SIRT2 결핍 마우스에서 크게 약화되었다. 게다가, 고농도 산소에 노출되었을 때 SIRT2 결핍 마우스는 야생형 마우스보다 TUNEL 양성 세포, 세포 독성, 카스파제 활성화 및 세포사멸 촉진 분자 발현이 감소한 것으로 나타났다. 더 나아가, 고농도 산소 노출 후 FOXO3의 아세틸화는 SIRT2의 결핍 시 증가하였으며, SIRT2는 세포사멸과 관련된 FOXO3의 표적 유전자인 BIM, PUMA, PERP, AATF의 전사에 관여하였다. 마지막으로, SIRT2의 억제제인 AGK2를 투여하였을 때 고농도 산소로 인한 염증 및 세포사멸 정도가 약화되었다.

**결론** : 본 연구에서는 SIRT2가 FOXO3의 탈아세틸화를 통해 세포사멸 신호 전달을 조절함으로써 고농도 산소로 인한 급성 폐 손상의 발병에 중요한 역할을 한다는 것을 밝혔다. 이러한 발견을 통해 SIRT2가 고농도 산소로 인한 급성 폐 손상의 병인 기전에 대하여 새로운 치료 전략을 제공할 수 있음을 나타냈다.

---

**핵심되는 말** : 급성 폐 손상, 세포사멸, 탈아세틸화, FOXO3, 고농도 산소, SIRT2